International Journal of Archaeology
2026, Vol. 14, No. 1, pp. 5–15
https://doi.org/10.11648/j.ija.20261401.12

SciencePG
Science Publishing Group

Research Article

Assessing Unmarked Graves Using Ground-penetrating Radar at Ayn Gharandal Archaeological Site, Jordan

Abdelrahman Aqel Abdelrahman Abueladas*, Omar Ahmad Mohamed Al-Bayari

Civil Engineering Department, Al-Balqa Applied University, Al-Salt, Jordan

Abstract

Ground-penetrating radar (GPR) has emerged as a valuable non-invasive technique for detecting and delineating unmarked graves, particularly in arid and semi-arid environments where preservation conditions differ markedly from humid settings. The Islamic religion forbids excavating graves or moving human remains, as such, GPR represents an effective method to determine grave characteristics including burial depth, size, type, and orientation of caskets, as well as the distribution and number of graves within a particular area. This study evaluates the effectiveness of GPR in identifying subsurface grave features within dry climate regions, where low soil moisture, limited vegetation cover, high electrical resistivity, and minimal organic decomposition can influence radar signal behavior. Grave characteristics including depth of burial, size, type, and orientation of caskets, as well as the quantity of graves in a given region and the geographic distribution of burials within a particular area, may frequently be ascertained using (GPR). In this study, two unmarked grave sites were surveyed using a SIR-20 GSSI (GPR) instrument. The number of graves and precise locations were unknown due to the lack of historical information. GPR data were acquired using multiple antenna frequencies to optimize the balance between radar penetration depth and resolution. Two anomalies representing possible unmarked adult graves and one unmarked infant grave were identified by two-dimension two-dimension (B-scan) and three -dimensions (C-scan) cross –sections. The anomalies ranged from 0.6 to 1 meters in depth, with lateral dimensions of 0.6 to 2 meters is typical for individual burials. All mapped anomalies have northwest-southeast orientation consistent with Islamic burial practices.

Keywords

Ayn Gharandal, Unmarked Graves, Ground Penetrating Radar, Three Dimensions

1. Introduction

Excavation and probing techniques have often proven to be unreliable for locating unmarked graves. Many long-standing graves no longer have headstones or footstones, which are frequently moved, or in poor condition. As a result, use of geophysical methods like GPR to map buried human remains is growing in both archaeological and forensic environments [8, 19, 22, 26]. Tens to hundreds of years old burials have been successfully located in archaeological studies [15-17, 25].

Geophysical techniques have been widely applied to locate mass burials and unmarked graves in both modern and pre-historic contexts [7-10, 14, 16, 32, 34]. The identification of unmarked graves in cemeteries associated with murder investigations, war crimes,

*Correspondence: Abdelrahman Aqel Abdelrahman Abueladas (aabueladas@bau.edu.jo)

Received: 13 March 2026; **Accepted:** 31 March 2026; **Published:** 13 May 2026

and humanitarian inquiries, including both mass and individual burials, is a common forensic application [27, 29, 33]. Although the use of geophysical methods in forensic and archaeological grave searches is increasing, some investigations have been compromised by misleading anomalies [6, 12].

GPR detects unmarked graves by identifying contrasts in subsurface physical properties that are influenced by soil moisture, texture, porosity, and the presence of conductive fluids or solids [7-9, 14, 16, 32, 34].

Grave excavation and refilling alter soil porosity, compaction, and grain sorting, creating subsurface contrasts that can be detected using GPR [19, 24].

The typical grave is made up of the grave fill, grave cut, grave, remains, shaft and sometimes a burial container [22]. These features generate physical property contrasts that are potentially detectable using geophysical methods [7, 16]. However, radar responses from graves can vary considerably depending on burial depth, age, soil composition, moisture conditions, and decomposition processes [1, 15].

In Islamic religion, excavation of graves or disturbance of human remains is prohibited. Consequently, non-invasive and non-destructive methods such as GPR provide an effective approach for locating potential unmarked graves with-out disturbing burial sites. The objective of this study is to evaluate GPR signatures associated with unrecorded and unmarked graves in a sandy, arid continental climate.

1.1. Study Area

The Wadi Gharandal region experiences extremely hot summers and moderate winters. During (June–September), average daily maximum temperature can frequently reach 37°C with a mean daily range of 12°C, while winter (November–March), the average daily temperature ranges from 17 to 26°C, with nighttime lows below 9°C. The average annual precipitation is approximately 66 mm almost exclusively during the winter Relative humidity ranges from 35% to 60%.

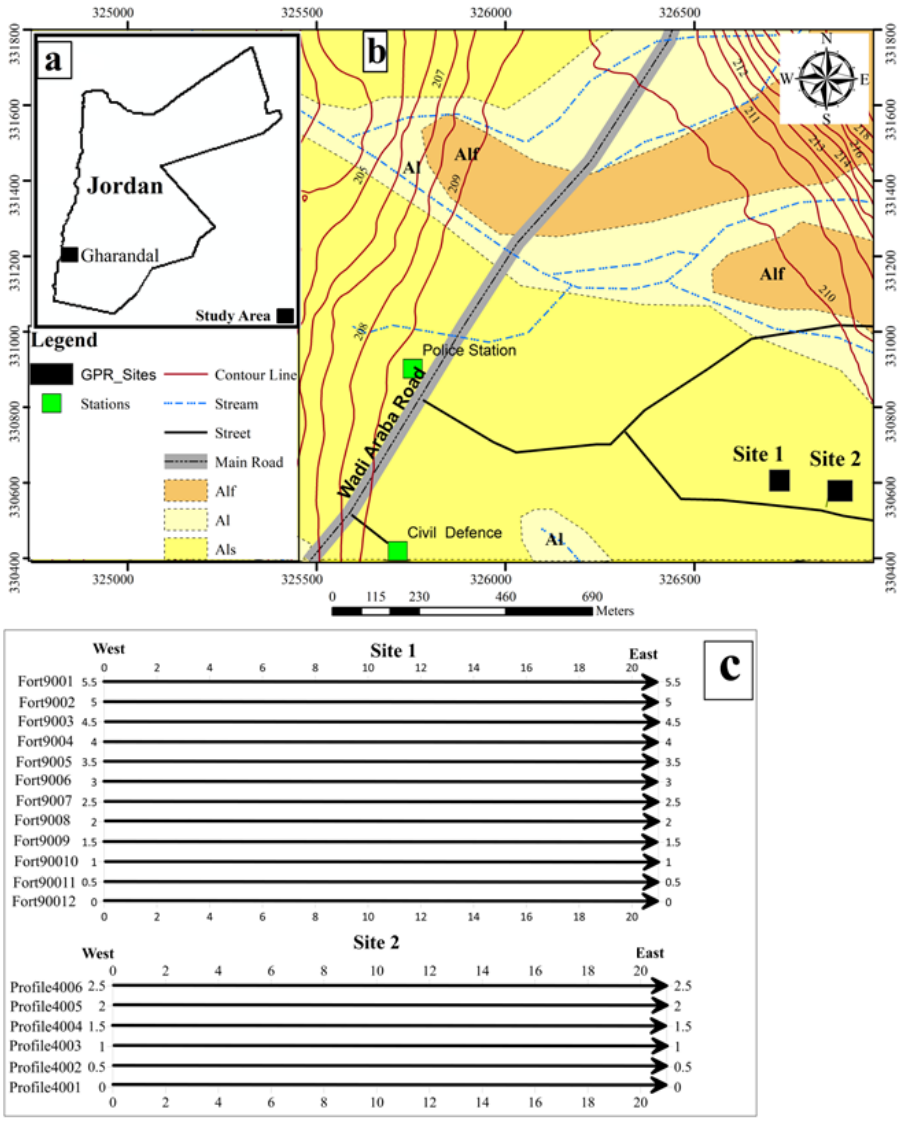

Figure 1. *Location map of the study area and the locations for GPR site 1 and 2.*

The Ayn Gharandal archaeological is located on the eastern margin of Wadi Arabah, approximately 200 m west of the entrance Wadi Gharandal 100 km north of the Gulf of Aqaba and 40 km southwest of Petra (WGS84 Coordinates: N 30°05.187', E 35°12.209') [4, 13] (Figure 1a). The site includes remains of a the Late Roman castle, bathhouse, and aqueduct system and additional unnamed buildings situated on steep cliffs overlooking the wadi system [14].

The study comprises multiple transects across two target sites and is about 1 km east of Jordan Valley Highway 65 and 200 m south-west of the Ayn Gharandal archaeological site. Surface geology comprises Quaternary deposits, including alluvial fans (Af) composed of gravel, sand, silt and Alluvial/Aeolian sand (Als), wadi sediments (Al) consisting of poorly to well-sorted matrix- and clast-supported layers [28] (Figure 1b).

1.2. GPR Method

GPR is a high resolution technique that uses electromagnetic waves with a frequency range of 10MHz–2GHz to image subsurface objects. Pulsed electromagnetic occurring at interfaces with contrasting electrical resistance. These reflections can be used to map anomalies which often indicate buried objects and stratigraphic disturbances in the shallow subsurface.

A GPR system records reflected energy as one-dimensional amplitude traces (A-scans) (Figure 2a), which are assembled into two-dimensional vertical profiles (B-scans) (Figure 2b). Interpolated B-scans generate horizontal time- or depth-slice images (C-scans) (Figure 2c), enabling three-dimensional visualization of subsurface features [11, 31, 37].

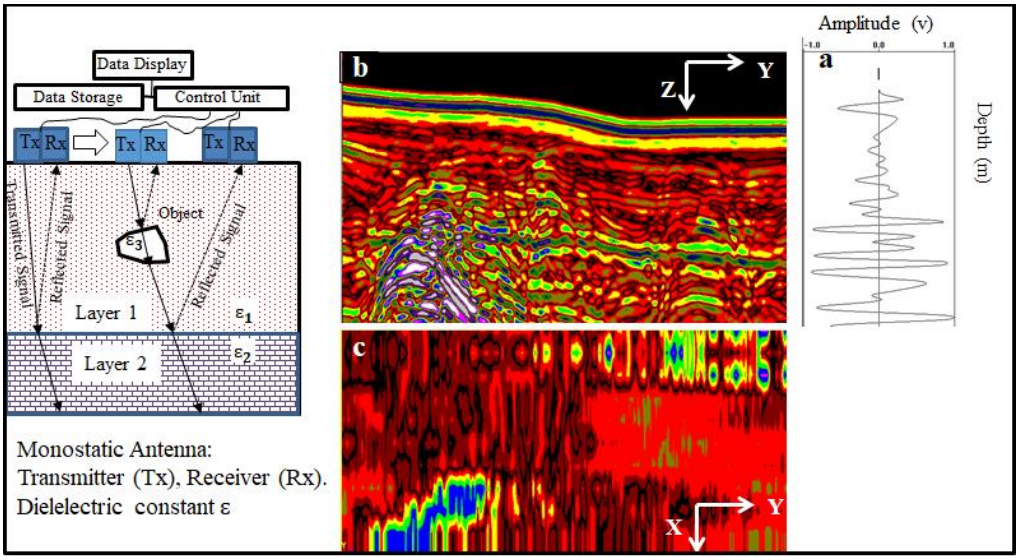

Figure 2. *Principles of ground penetrating radar (GPR). a) A-scans displayed varying amplitude with time or depth (vertical). (b) B-scan; a vertical 2D cross-section of stitched together A-scans; also known as "transects" or "plan view." (c) C-scan; a horizontal 2D cross-section of interpolated B-scans; also known as "depth slices" or "time slices" which is subtract from 3D section.*

Vertical resolution is controlled by wavelength (λ) and velocity (v) and improves with increasing frequency (f) as seen in Equation (1) [3, 29]:

$$\lambda = v/f \quad (1)$$

The optimal vertical resolution is approximately one-quarter can of the dominant wavelength [3, 30, 38].

1.3. GPR Survey

A Geophysical Survey Systems, Inc. (GSSI) SIRvoyer-20 was used to conduct a continuous GPR survey, with antennas operating at frequencies of 400 MHz and 900 MHz. Eighteen profiles to totaling approximately 360 m were collected at two sites (Figure 1c). Parallel profiles were spaced at 0.5 m intervals to constrain anomaly dimensions and orientations (Figure 1c). Parallel profiles were spaced at 0.5 m intervals to constrain anomaly dimensions and orientations.

Site 1 situated about 100 m west of Gharandal historical site and Site 2 is located about 80 m east of the archeological site. The study areas were selected for the flatter topography with open-fields and scattered bushes and rocks.

1.4. GPR Processing

Data processing was completed using The GSSI RADAN VII software. To enhance the radar cross- section resolution and remove extraneous noise, different signal parameters and

filters were applied, including time- zero correction, background removal, surface normalization, gain functions, band pass filtering and Kirchhoff migration [3].

The Kirchhoff Migration was applied as a preparatory processing step, with the relative velocity automatically specified in the processing program. Phantom reflections resulting from data migration or employing the wrong migration settings, were identified and removed [20, 22].

The migration process smoothed the traces, reduced the unwanted surface pulses and reflections, and produced a more unified representation of the anomaly and constrained the anomaly's location [35, 36, 39] (Figure 3).

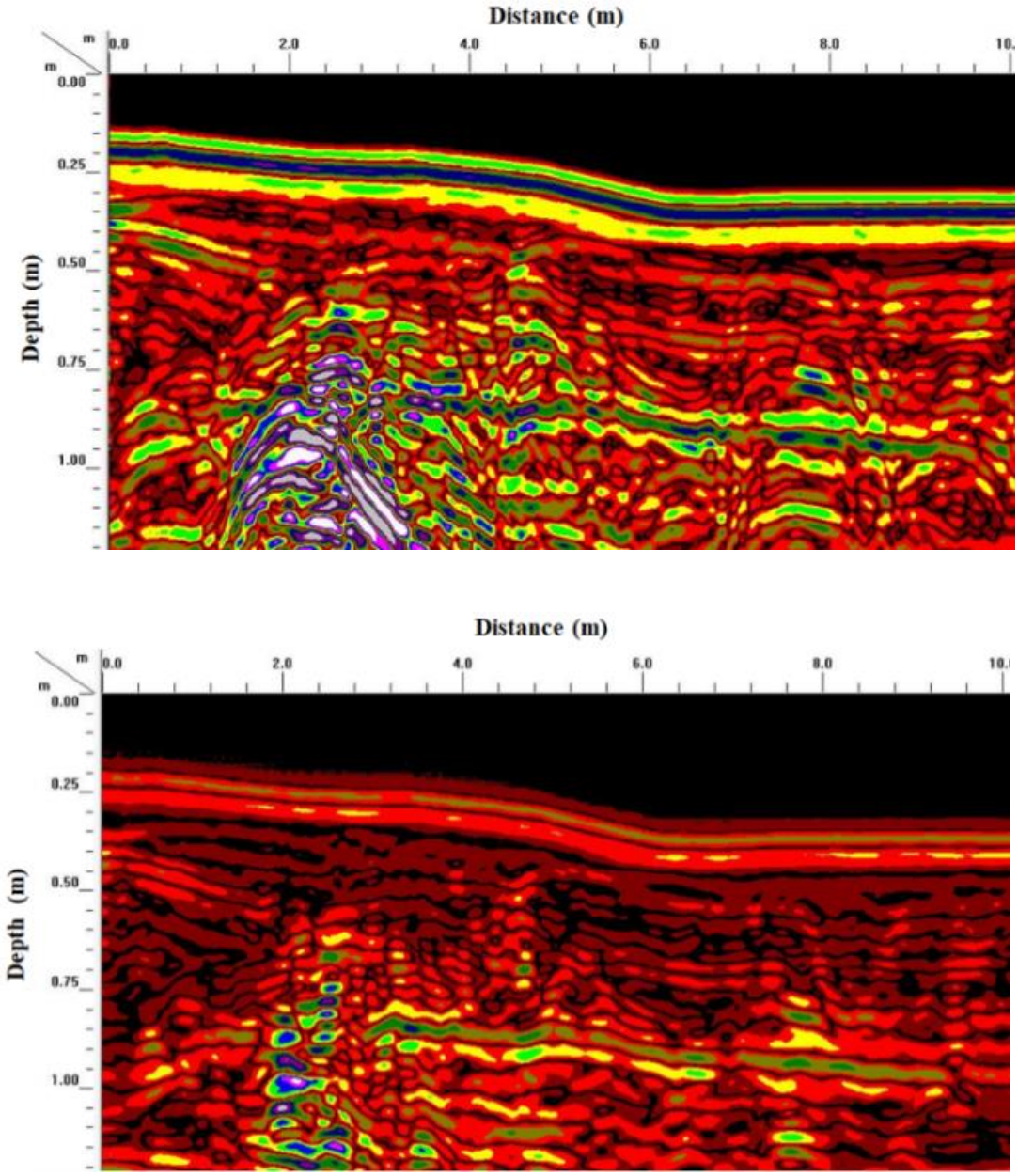

Figure 3. *GPR profiles Fort9003 before and after migration.*

A soil type calibration is required to achieve a precise depth axis and accurate target depth calculation in a GPR radargram.

The two-way travel time of the reflected signal is converted actual depth of the reflector by calculating the subsurface radar-wave velocity [5, 15]. In this study, velocity calibration were performed using buried linear pipe oriented 90° to the survey direction to produce a well-defined target hyperbola suitable for the soil type calibration.

An approximation of the reflection delay formula, which links wave velocity (v) to measured depth (x), recorded relative permittivity (ϵr), two-way travel time (t), and free-space velocity (c), was used to determine the dielectric permittivity at different locations [3, 21]:

$$\varepsilon_r = (c/v)^2 = (c\ t/2x)^2 \quad (2)$$

The near surface average velocity was determined to be 0.14 m ns^{-1}.

2. Results

The GPR data revealed a number of subsurface anomalies consistent with potential unmarked individual grave features.

GPR profiles from the combined 400MHz and 900 MHz frequency antennae, identified multiple hyperbolic reflection anomalies consistent with unmarked graves at both Site 1 (Figure 4a) and Site 2 (Figure 5a and Figure 6).

At site 1, a distinct hyperbolic anomaly is present in both the 400MHz and 900 MHz frequency antenna indicative of a possible unmarked grave at a depth of around 0.8 m. There is a distinct dielectric contrast reflection hyperbolic pattern between 1.5 to and 2 m horizontally and 0.8 to 1.8 meters vertically along Fort9003 (Figure 4a). A similar anomaly with both matching distance and depth can be signed along the 400 MHz antenna radargram profile Fort4003 which sited at the line [2] (Figure 4b).

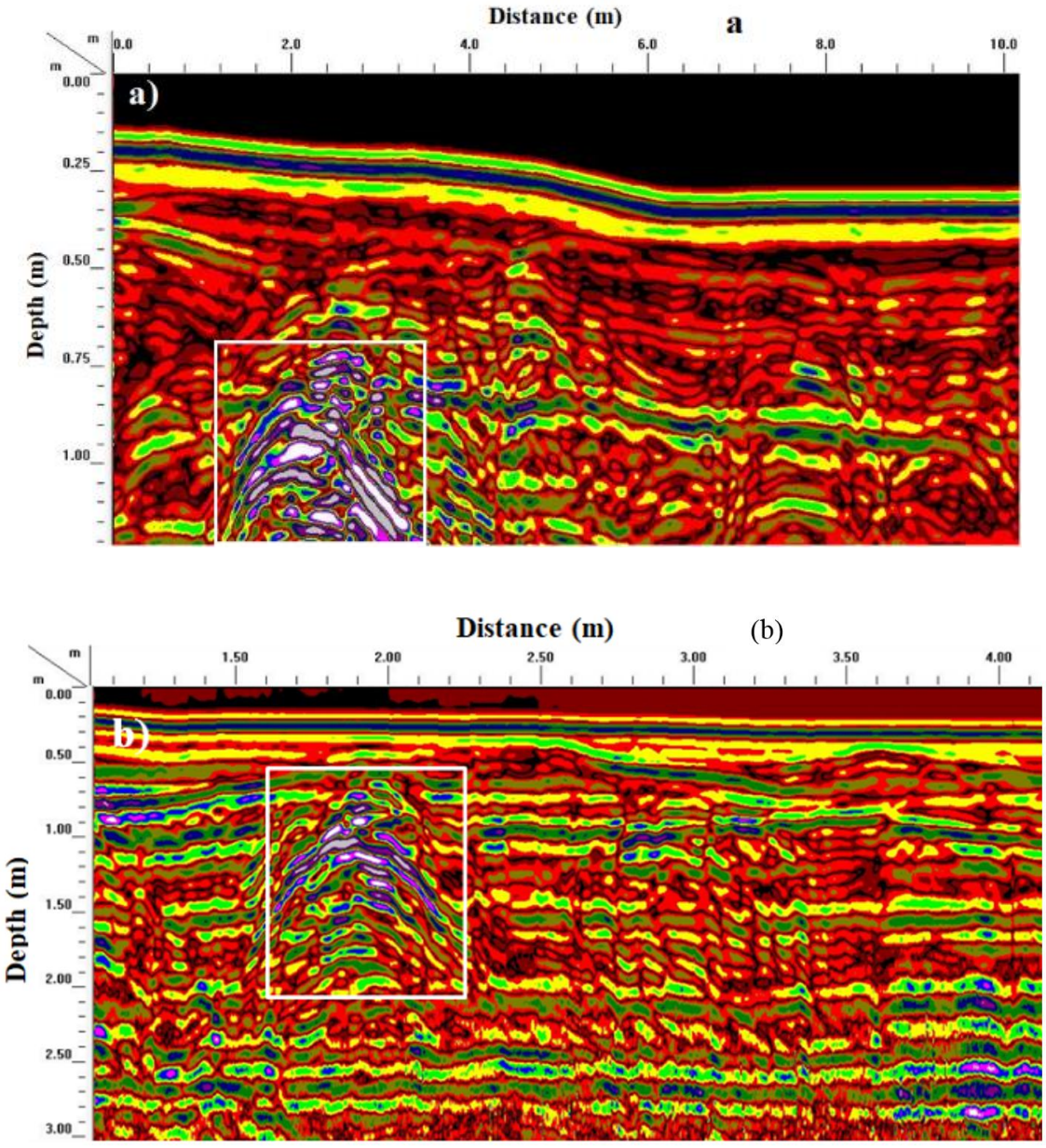

Figure 4. *A distinct anomaly, bracketed within the white rectangle. a) A portion of 900 MHz radargram along profile FORT9003 at site 1. The hyperbolic shape anomaly situated at distance between 1.5 m to 2 m and 0.8 to 1.8 m deep, shows a possible grave. b) The same anomaly can be observed along 400 MHz radargram FORT4003 which has the same location as FORT9003.*

At site 2, two anomalies are observed in the section along profile4004. The 400 MHz antenna radargram shows two hyperbolic-shaped anomalies, located between 10.5 m to 13.5 m horizontally and approximately 0.8 to 1.7 m vertically and 18 m approximate depth of 1.1 m, respectively.

The first anomaly may indicate a possible grave, and the second anomaly may represent buried rock or a boulder (Figure 5a). Figure 5b shows the profile 4004 migrated section.

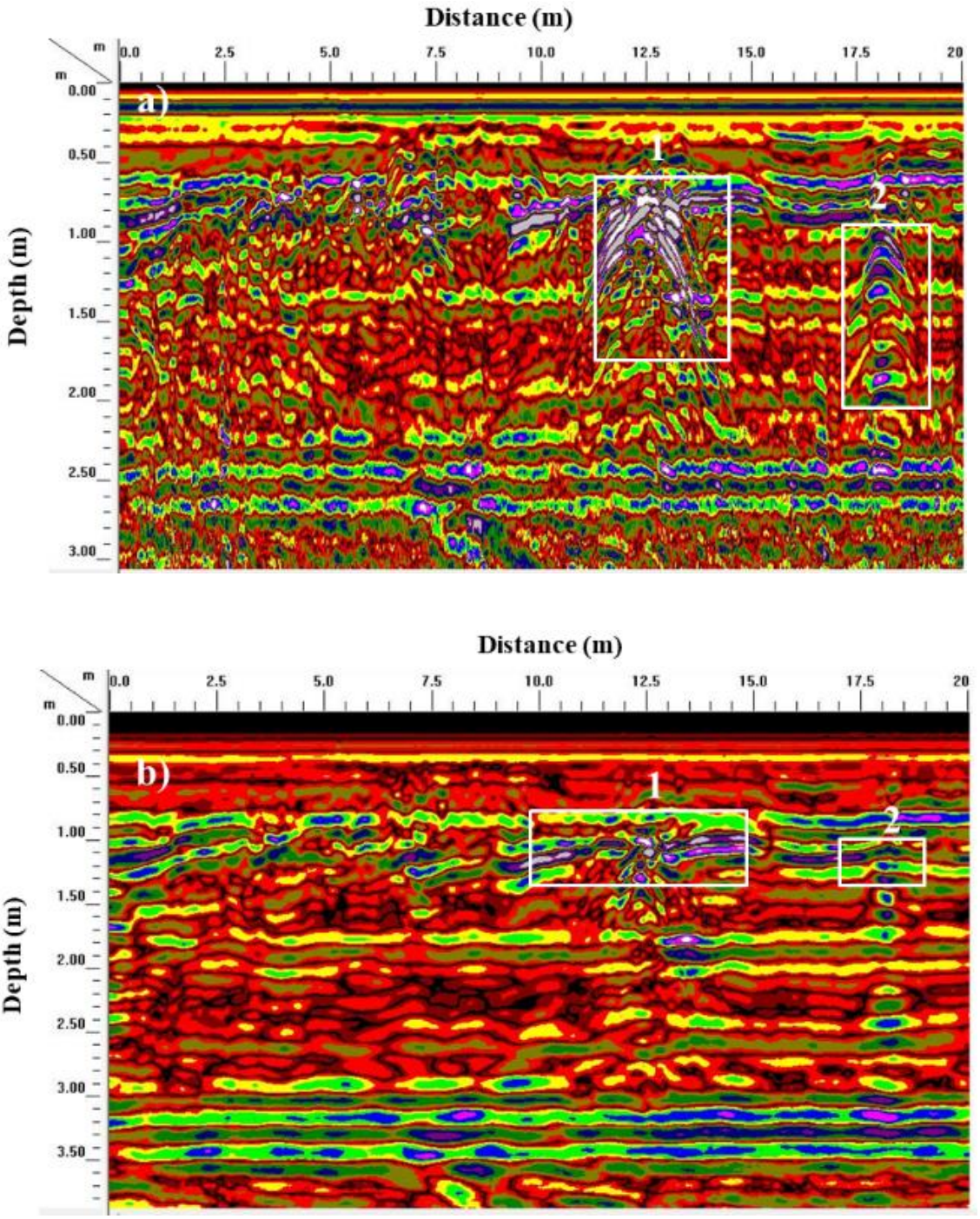

Figure 5. *a) A portion of 400 MHz radargram along profile 4004 at site 2. The hyperbolic anomaly at 12.5 m to 0.8 m deep shows a possible grave, the second anomaly at distance 18 m and 1 m deep shows a possible rock. b) The profile 4005 migrated section.*

Figure 6 illustrates data collected from the first 15 m along profile 4005 showing two hyperbolic shape anomalies, the first between 7.5 to 9 m, the second between 11m to 13.5 m. The second anomaly seems to be an extension of the first hyperbolic anomaly along profile 4004.

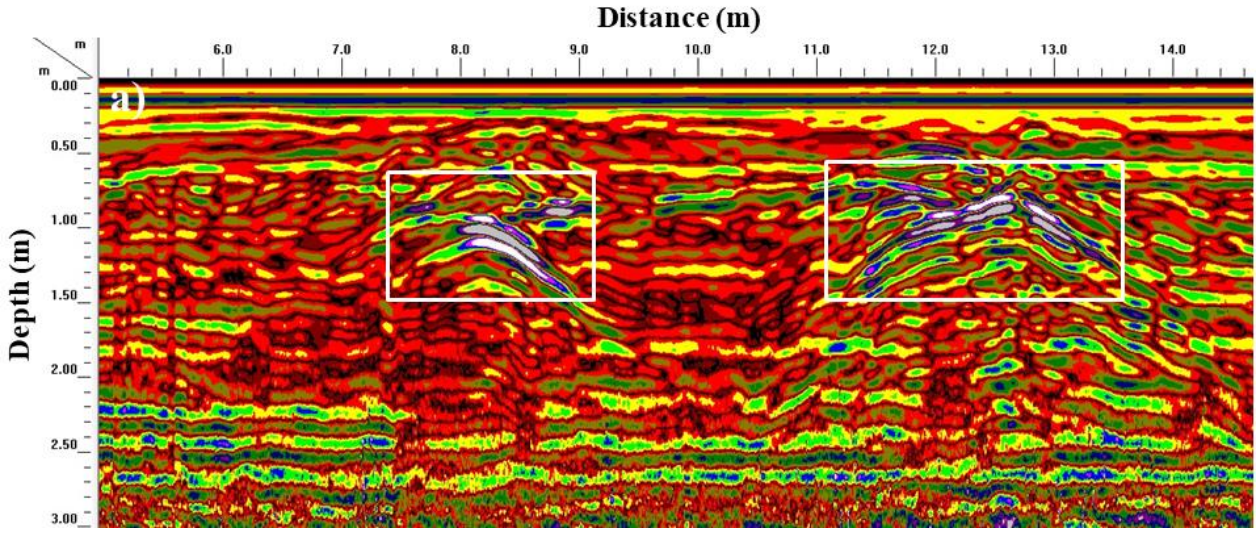

Figure 6. *A portion of 400 MHz radargram along profile 4005. Two hyperbolic shape anomalies appear at distance between 7.5 to 9 m and 11 to 13.5 m respectively.*

The migrated section is shown in Figure 7. As seen within the white rectangles, the layers are discontinuous and fragmented along sections of the line between distance 8 to 9 meters, and 11.5 to 13 meters respectively, which is to be expected if a grave was excavated and then refilled at this location (Figure 7).

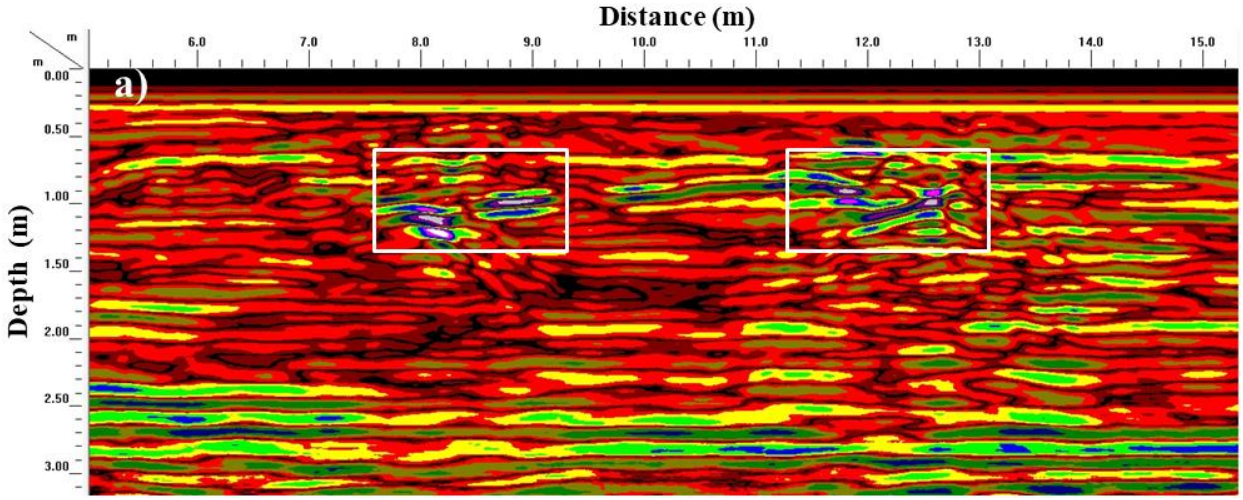

Figure 7. *A portion of GPR profile 4005 migrated section. A distinct anomaly is highlighted within within the white rectangle.*

The anomaly's precise geometry can be distinguished by arranging the 2D images or B-scan slices into a three-dimensional (3D) or C-scan image, which is highly helpful for analyzing graves [17, 18, 23, 31].

At site 1, parallel GPR 900 MHz profiles were used to create amplitude slice maps at specific horizontal strata in order to carry out map the area in 3D (Figure 1C).

In contrast to visually identifying numerous reflections within each radar profile, the amplitude slice-map or C-scan method generally more time-efficient and accurate. A 3D representation is produced by combining multiple parallel B-scan profiles in x and y plane, enabling visualization of both plan and cross-sectional views through 3D processing [2] (Figure 8).

Figure 8 shows a 3D section (chair view) with x =2: 5, y =0, with depths 0.8, 1 and 1.27 m bellow the earth surface is shown the possible potential grave anomaly observed with NW-SE direction and appears in three depth slices in the (C-scans) display.

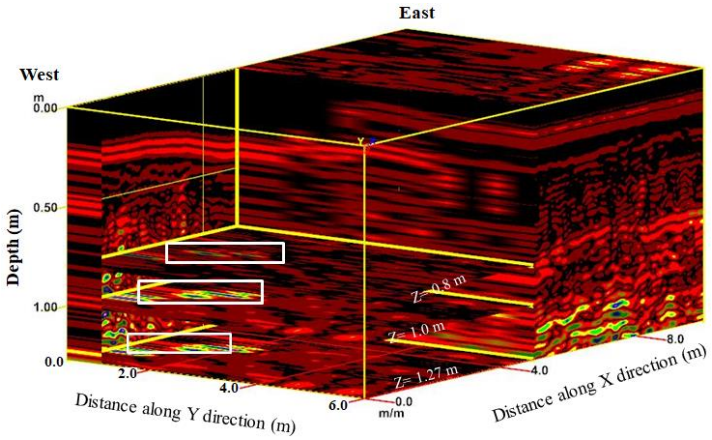

Figure 8. *The 3D section (chair view) with x =2: 5, y =0, and different slides depth 0.8, 1 and 1.27 m bellow the ground surface shows the possible grave location (white rectangle).*

Figure 9 shows multiple parallel slices (C-scan) at distance (0, 2, 3.5, and 6) along the y direction. The anomaly can be seen at distance 0, 2, 3.5m and cannot be seen in slides 4 and 6.

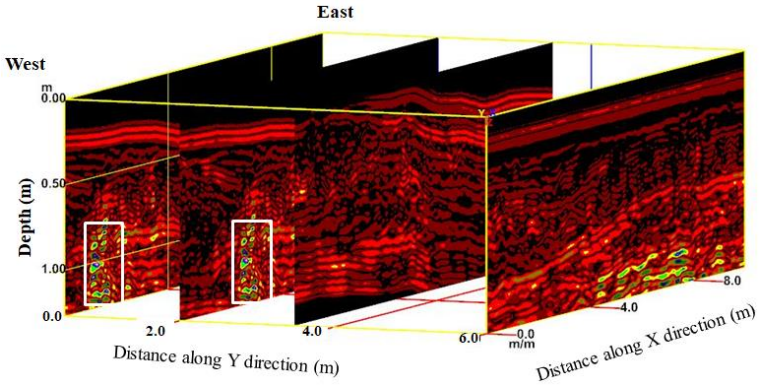

Figure 9. *Time slice y-cut display (C-scan) at distance (0, 2, 3.5, and 6 m) determines the location of the possible grave (white rectangle).*

At site 2, the C-scan constructed from 2D- 400 MHz parallel profiles at (0.75, 1.2 and 2 m) depths are shown in Figure 10.

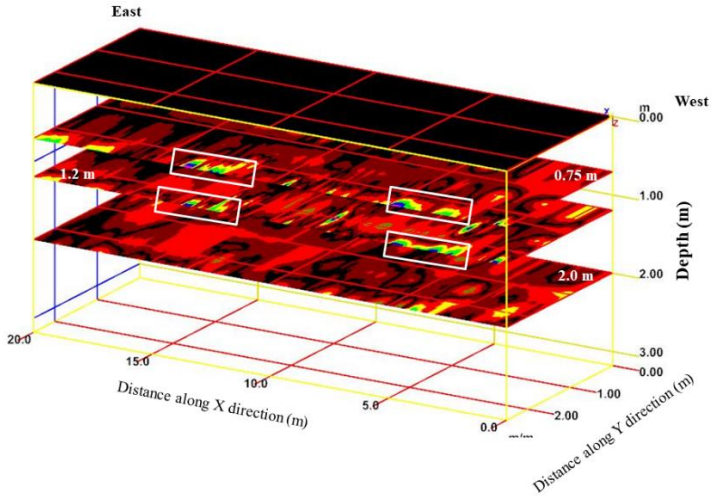

Figure 10. *Site 2 400 MHz multi slices (C-scan) view at depths of 0.75, 1.2 and 2 m bellow the ground surface shows the possible two graves location (white rectangle).*

3. Discussion

Compared to other techniques, GPR data is frequently thought to be more complex [11, 20, 22] partly because of the subtleties of data processing, but also because of how many items GPR can identify.

GPR was used at the study area due to the lack of historical and geophysical data in the study area and to avoid physical excavation to location unmarked graves. When surveying a location suspected of having unmarked graves, GPR can be used to create real-time, onscreen 2D GPR (B-scan) images, which can be used to inform decision-making and guide investigations.

At two surveyed sites both 400 MHz and 900 MHz GPR antennas were effective for detecting shallow possible grave, as both antennas have good detection of the simulated possible graves, also having sufficient penetration depths. The B-scan profiles showed one isolated hyperbolic reflection anomaly at site 1 and two isolated hyperbolic reflection anomalies at site 2.

3D visualization of a GPR scan can improve anomaly detection capabilities 3D C-scans, in contrast to B-scans, provide a wholistic interpretation of the subsurface indicative of likely burial. In the study areas, the discontinuous and fragmented layers mapped across multiple parallel sections suggest an unmarked grave with a horizontal distance between 1 and 2 m and an approximate depth of 0.8 m. The spatial relationships across the sections allow for differentiation between likely graves and natural features such as rocks, like the anomaly located at site 2. Graves are shown in multiple profiles which can be correlated while individual rocks are observed in only one reflection profile located at site 2 and not on the parallel profiles.

4. Conclusion

To identify and map potential burials at the Gharandal sites, GPR scans using antennas with frequencies ranging from 400 to 900 MHz, This frequencies provide sufficient resolution for detecting subsurface feat at depths around 3 m and 1 m, respectively. Tree roots, burrows and rocks can be discriminated from human burials because they will produce extended and sinuous shaped reflections or be observed in a single profile, whereas graves produce spatially distinct hyperbolic anomalies dimensions consistent with a human body, whether an infant or adult.

At site 1 lateral extent and width of the mapped hyperbolic reflection anomaly with both antennae consistent with an adult grave. All interpreted grave features occurred at depths ranging from 0.6 to 1 m with lateral dimensions 0.6 to 2 m. The northwest-southeast orientation is consistent with Islamic burial practices. While GPR surveys are effective for identifying subsurface disturbances, voids and spatial distribution pattern, they cannot confirm the presence of human remains.

Acknowledgments

We would like to express our thanks to the Dean of Faculty of Engineering and the chair of Civil Engineering Department and all our colleagues for their corporation and support.

We are also grateful to the crews of the Al-Balqa Applied University Eng. Hisham Awamleh, Yousef Al-Faory for their assistance throughout radar data acquisition and processing. We are grateful to the editor and the anonymous reviewers for their helpful comments and recommendations on this work.

Abbreviations

GPR Ground-Penetrating Radar

Author Contributions

Abdelrahman Aqel Abdelrahman Abueladas: Conceptualization, Data curation, Formal Analysis, Resources

Omar Ahmad Mohamed Al-Bayari: Supervision, Writing – original draft

Conflicts of Interest

The authors declare no conflicts of interest.

References

[1] Abbas M., Ghazala H., Hany S. Mesbah H. S., Atya M., Radwan A., Hamed D. A. Implementation of ground penetrating radar and electrical resistivity tomography for inspecting the Greco-Roman Necropolis at Kilo 6 of the Golden Mummies Valley, Bahariya Oasis, Egypt. NRIAG Journal of Astronomy and Geophysics. 2016, 5, 147–159. http://dx.doi.org/10.1016/j.nrjag.2016.01.003

[2] Abueladas, A. A., and Akawwi E.. Ground-penetrating radar inspection of subsurface historical structures at the baptism (El-Maghtas) site, Jordan. Geoscientific Instrumentation, Methods and Data Systems. 2020, 9(2), 491-497. https://doi.org/10.5194/gi-9-491-2020

[3] Abueladas, A. A. Assessment of seismic hazards along the northern Gulf of Aqaba, PHd thesis, University of Missouri Kansas City. 2014, 135. https://ui.adsabs.harvard.edu/abs/2014PhDT121A/abstract

[4] Allison A. Paleoseismology and Archaeoseismology along the Southern Dead Sea Transform in Wadi 'Arabah Near the municipality of Aqaba, Jordan. UMKC Dissertation. 2013. https://mospace.umsystem.edu/items/2ae0653e-daa5-4b69-a017-e673cf78685c

[5] Annan, A. P. Electromagnetic principles of ground penetrating radar. In Ground penetrating radar: Theory and applications Elsevier Science. 2009, 1–40. https://doi.org/10.1016/B978-0-444-53348-7.00001-6

[6] Annan, A. P. 2002. GPR History, Trends, and Future Developments. 2002, 3, 253–270.

[7] Berezowski, Mallett V., Ellis J., Moffat I. Using ground penetrating radar and resistivity methods to locate unmarked graves: a review, Remote Sens. 2021, 13, 15 https://doi.org/10.3390/rs13152880

[8] Bevan, B. W. The search for graves, Geophysics. 1991, 56(9), 1310–1319, https://doi.org/10.1190/1.1443152

[9] Cheetham, P. Forensic Geophysical Survey. In: Hunter, J. and Cox, M., eds. Forensic Archaeology [online]. Abingdon-on-Thames: Routledge, 2005, 62–95. https://www.taylorfrancis.com/books/9780203970300 [Accessed 10 Nov 2017].

[10] Cristino, K., Doro, K., Armstrong, A., Forbes, Sh, Gayon, A., Georg Bank, C. Electrical resistivity tomography of simulated graves with buried human and pig remains. Forensic Science International. 2024, 364, 1-11. https://doi.org/10.1016/j.forsciint.2024.112248

[11] Conyers, L. B. Interpreting Ground-Penetrating Radar for Archaeology. Taylor & Francis, UK, London. 2012.

[12] Dalan, R. A., De Vore S. L., Clay R. B.. Geophysical identification of unmarked historic graves, Geoarchaeology. 2010, 25(5), 572–601. https://doi.org/10.1002/gea.20325

[13] Darby, R. and Darby E. The Late Roman fort at 'Ayn Gharandal, Jordan: interim report on the 2009–2014 field seasons, Journal of Roman Archaeology. 2015, 28(1), 461-470. https://doi.org/10.1017/S1047759415002603

[14] Davis, J. L., Heginbottom J. a., Annan A. P., Daniels R. S., Berdal B. P., Bergan T., Duncan K. E.,, Lewin P. K., Oxford J. S., Roberts N., Skehel J. J., Smith C. R. Ground Penetrating Radar Surveys to Locate 1918 Spanish Flu Victims in Permafrost. Journal of Forensic Sciences. 2020, 45(1), 68–76. http://www.ncbi.nlm.nih.gov/pubmed/10641921

[15] Dick, H. C., Pringle J. K., Wisniewski K. D., Goodwin J., van der Putten R., Evans G. T., Francis J. D., J. P. Cassella, J. D. Hansen (2017). Determining geophysical responses from burials in graveyards and cemeteries, GEOPHYSICS. 2017, 82(6), B245–B255. https://doi.org/10.1190/geo2016-0440.1

[16] Everett M. E., Bowling J. T., Dees R. Radar diagnostic testing for classification of unmarked graves. Discover Applied Sciences. 2026, 8, 137, 3-29. https://doi.org/10.1007/s42452-025-07949-4

[17] Fisher, E. Examples of reverse-time migration of single-channel, ground penetrating radar profiles: Geophysics. 1992, 57(4), 577-586. https://doi.org/10.1190/1.1443271

[18] Gaber, A. El-Qady G., J., Khozym A., Abdallatif T., Kamal S. Indirect preservation of Egyptian historical sites using 3D GPR survey. Egypt. J. Remote Sens. Space Sci. 2017, 21, S75–S84. https://doi.org/10.1016/j.ejrs.2017.11.004

[19] Gaffney, C., Harris C., Pope-Carter F., Bonsall J., Fry R., Parkyn A. Still searching for graves: An analytical strategy for interpreting geophysical data used in the search for "unmarked" graves, Surf. Geophys. 2015, 13(6), 557–569. https://doi.org/10.3997/1873-0604.2015029

[20] Goodman, D. and Piro S. GPR Remote Sensing in Archaeology. GPR Remote Sensing in Archaeology. 2013, Berlin: Springer-Verlag. https://books.google.jo/books/about/GPR_Remote_Sensing_in_Archaeology.html?id=wc1JAAAAQBAJ&redir_esc=y

[21] Gracia, F. G.,. Blanco M. R, Abad I. R., Sala R. M., Ausina I. T., Marco J. B., Conesa J. L. M. GPR technique as a tool for cultural heritage restoration: San Miguel de los Reyes Hieronymite Monastery, 16th Century (Valencia, Spain). Journal of Cultural Heritage. 2007, 8, 87–92. https://doi.org/10.1016/j.culher.2006.10.005

[22] Green, A. Detecting graves in GPR data: assessing the viability of machine learning for the interpretation of graves in B-scan data using medieval Irish case studies. Doctoral Thesis (Doctoral). 2020, Bournemouth University. P. 1.

[23] Halim, N., Abdullah N., Ghazali M. D., Hassan H. The Possibility of Using Terrestrial-Based Ground Penetrating Radar (GPR) Technology for Supplying 3rd Dimension Information for a Search and Recovery Mission for Landslide Victims International Journal of Geoinformatics. 2022, 19(5), 105–118.

[24] Hammon W., McMechan G., Zeng X. Forensic GPR: finite-difference simulations of responses from buried human remains. Journal of Applied Geophysics. 2000, 45(3), 171-186. https://doi.org/10.1016/S0926-9851(00)00027-6

[25] Hanninen, P. and S. Autio. Fourth International Conference on Ground Penetrating Radar. 1992, 359–365.

[26] Henry E. R., Wright A. P., Sherwood S. C., Carmody S. B., Barrier C. R., Van de Ven C. Beyond Never-Never Land: Integrating LiDAR and Geophysical Surveys at the Johnston Site, Pinson Mounds State Archaeological Park, Tennessee, US. 2020, 12, 2364, 1: 30. https://doi.org/10.3390/rs12152364

[27] Jasinski, M. E., A. Ossowski, K. Spradley (2023). Uncovering war crimes: hidden graves of the Falstad forest, Herit. Mem. Confl. 2023, 3, 19–24. https://doi.org/10.3897/hmc.3.94923

[28] Khalil, I. Geology Directorate Geological Mapping Division BULLETIN 24, Amman 1993, 1: 50,000 Geological Mapping Series. The geology of Wadi Gharandal area, map, 1993, sheet NO. 3050 II.

[29] Knapp, R. W. (1990). Vertical resolution of thick beds, thin beds and thin-bed cyclothems: Geophysics. 1990, 55, 1183-1190. https://doi.org/10.1190/1.1442934

[30] Knight, R., Tercier P., Irving J. The effect of vertical measurement resolution on the correlation structure of a ground penetrating radar reflection image. Geophysical Research Letters. 2004, 31, L21607: 1-4. https://doi.org/10.1029/2004GL021112

[31] Martin J., Everett, M. A methodology for the self-training and self-assessing of new GPR practitioners: Measuring diagnostic proficiency illustrated by a case study of a historic African-American cemetery for unmarked graves. Archaeological Prospection. 2023, 3, 311-325. https://doi.org/10.1002/arp.1893

[32] Mellett, J. S. Location of human remains with ground-penetrating radar. In P. Hanninen & S. Autio (Eds.), Fourth International Conference on Ground Penetrating Radar, Special Paper. Geological Survey of Finland. 1992, 16, 359-365. Espoo https://doi.org/10.3997/2214-4609-pdb.303.45

[33] Meyer C., Carletti M., Sala R., Simón P. R., Jerlagic S., Kapsali K., Dias., Ruivo J., da Silva R. C., Correia V. H. Conimbriga: A Comprehensive Geophysical Survey and the Reconstruction of the Town's Plan. Open Archaeology. 2026, 12(1), 20250068. https://doi.org/10.1515/opar-2025-0068

[34] Mohapatra, S. and McMechan G. A. Prediction and subtraction of coherent noise using a data driven time shift: A case study using field 2D and 3D GPR data. J. Appl. Geophys. 2014, 111, 312–319. https://doi.org/10.1016/j.jappgeo.2014.10.018

[35] Patterson, J. E, and Cook, F. A. Successful application of ground-penetrating radar in the exploration of gem tourmaline pegmatites of southern California. Geophysical prospecting. 2002, 50, 2, 107-117.

[36] Pringle, J. K., Ruffell A., Jervis J. R., Donnelly L., McKinley J., Hansen J., Morgan R., Pirrie D. and Harrison M. The use of geoscience methods for terrestrial forensic searches, Earth-Sci. Rev. 2012, 114(1), 108–123. https://doi.org/10.1016/j.earscirev.2012.05.006

[37] Sarris, A, Dunn R. K., Rife J. L., Papadopoulos N., Kokkinou E., Mundigler C. Geological and geophysical investigations in the Roman cemetery at Kenchreai (Korinthia), Greece. Archaeological Prospecting. 2007, 14(1), 1-23. https://doi.org/10.1002/arp.280

[38] Sheriff, R. E. (1977). Limitations on resolution of seismic reflections and geologic detail derivable from them: Applied geophysics. 1977, 20, 3-14. https://doi.org/10.1306/M26490C1

[39] Trung D., Giang N., Van N. The Application of Depth Migration for Processing GPR Data. E3S Web Conf. 2018, 35, 03004. https://doi.org/10.1051/e3sconf/20183503004